Development and Evaluation of a Leaf Disease Damage Extension in Cropsim-CERES Wheat

Georg Röll [1,*] , William D. Batchelor [2], Ana Carolina Castro [3,4], María Rosa Simón [3,5] and Simone Graeff-Hönninger [1]

[1] Department of Agronomy, Institute of Crop Science, University of Hohenheim, 70599 Stuttgart, Germany; Simone.graeff@uni-hohenheim.de

[2] Biosystems Engineering Department, Auburn University, Auburn, AL 36849, USA; wdb0007@auburn.edu

[3] Cerealicultura, Facultad de Ciencias Agrarias y Forestales, Universidad Nacional de La Plata, Av. 60 y 119, La Plata 1900, Argentina; ana.castro@agro.unlp.edu.ar (A.C.C.); mrsimon@agro.unlp.edu.ar (M.R.S.)

[4] Consejo Nacional de Investigaciones Científicas y Técnicas (CONICET), Centro Científico Tecnológico (CCT), La Plata 1900, Argentina

[5] Comisión de Investigaciones Científicas, Pcia. de Buenos Aires, 526, 10 y 11, La Plata 1900, Argentina

*   Correspondence: georg.roell@uni-hohenheim.de; Tel.: +49-711-459-22380

Abstract: Developing disease models to simulate and analyse yield losses for various pathogens is a challenge for the crop modelling community. In this study, we developed and tested a simple method to simulate septoria tritici blotch (STB) in the Cropsim-CERES Wheat model studying the impacts of damage on wheat *(Triticum aestivum* L.) yield. A model extension was developed by adding a pest damage module to the existing wheat model. The module simulates the impact of daily damage on photosynthesis and leaf area index. The approach was tested on a two-year dataset from Argentina with different wheat cultivars. The accuracy of the simulated yield and leaf area index (LAI) was improved to a great extent. The Root mean squared error (RMSE) values for yield (1144 kg ha^{-1}) and LAI (1.19 m^2 m^{-2}) were reduced by half (499 kg ha^{-1}) for yield and LAI (0.69 m^2 m^{-2}). In addition, a sensitivity analysis of different disease progress curves on leaf area index and yield was performed using a dataset from Germany. The sensitivity analysis demonstrated the ability of the model to reduce yield accurately in an exponential relationship with increasing infection levels (0–70%). The extended model is suitable for site specific simulations, coupled with for example, available remote sensing data on STB infection.

Keywords: wheat; disease; yield; septoria tritici blotch; leaf area index; crop modelling; decision support system for agrotechnology transfer (DSSAT); Cropsim-CERES Wheat

1. Introduction

Wheat *(Triticum aestivum* L.) is the second most important staple food crop for human nutrition. It is grown worldwide on approximately 220 million hectares under different climatic conditions. It is projected that wheat production must increase by 1.6% annually to meet the expected global demand by 2050 [1]. However, increasing temperatures and changing global rainfall patterns will likely influence breeding, management, fertilization and crop protection strategies for wheat [2] and also influence disease patterns [3,4]. Hence, crop protection measures will play an important role under future climate change, as rising temperatures and changes in rainfall pattern, will cause more favourable conditions for pests and diseases, especially in the warming north, where wheat production is predominant [2].

On a global scale, there are approximately 50 diseases and pests, which have the potential to damage wheat and reduce farmer's income [5–7]. On a global level, the most widely adapted wheat

fungal diseases are leaf rust caused by "*Puccinia triticina* E.," stripe rust caused by "*Puccinia striiformis* W.," stem or black rust caused by "*Puccinia graminis* E.," powdery mildew caused by "*Blumeria graminis* P." and septoria tritici blotch (STB) caused by "*Zymoseptoria tritici* D." [1]. The infection by "*Zymoseptoria tritici* D." is the most economically damaging wheat disease worldwide [8]. It can cause yield reductions of 50% to 60% [9] by creating leaf lesions resulting in defoliation and reduced photosynthesis. It has been estimated that 70% of the annual usage of fungicides in Europe is related to the treatment of this disease [10].

During the past decade, there has been an increasing resistance of STB to azole and strobilurin fungicides in Europe [9–11]. Breeding for STB disease resistance is complicated, due to the variability of the pathogen reproduction cycle [12,13]. Researchers have studied different strategies including tillage, crop rotation, delayed sowing, fungicide application and a proper level of fertilizer application to reduce or control the infection of STB [14]. It appears that moderate fungicide application coupled with the right amount of fertilizer is a strategy that holds promise for environmentally friendly wheat production, while reducing at the same time STB infection.

Crop models are suitable for decision support and contribute to a better understanding in the development of new wheat production strategies. They can play a vital role in understanding plant growth processes, the impact of different weather scenarios as well as management strategies on disease outbreak, final yield and grain quality. Hence, crop models might help to spread the production of wheat in more economic and sustainable ways.

Crop models can also provide an insight into yield losses due to pests and diseases, including STB. Several mechanistic wheat crop growth models have been developed over the last several decades, including APSIM [15], WheatGrow [16], STICS [17], Sirius [18] and DSSAT [19]. These models were developed to study crop-environment interaction and to evaluate optimum management strategies.

The Cropsim-CERES-Wheat (CCW) model [20–22] included in the DSSAT version 4.6 [23] was developed to study the impact of genetics, management, weather and climate change on wheat growth and yield. The model simulates daily plant development based on daily maximum and minimum temperature, daylength and vernalisation requirements. Growth is computed on a daily basis using a radiation use efficiency approach. Carbon is allocated daily to different plant parts based on the development stage. The CCW model has been linked with remote sensing data [24] and was successfully tested with different cultivars, soil characteristics as well as in different climatic conditions including Canada [25], Argentina [26], Southern Italy [27] and the United Kingdom [28]. Currently the CCW model does not account for damage due to weeds, pests or diseases [29]. As a consequence, inaccurate simulations of crop growth and yield result when simulating datasets that include pests and diseases [30,31].

Developing and incorporating a disease damage extension would expand the use of the CCW model to simulate and study the impact of disease damage on crop growth and yield. Batchelor et al. [32] incorporated a pest damage into the CROPGRO [33] family of models distributed with the DSSAT [34]. In their approach, they defined pest coupling points as daily rate and state variable modifiers to simulate the impact of daily pest damage on leaf, stem, seed, shell and root state variables and daily photosynthesis rate based on daily inputs of pest damage. They tested this approach for different pest damage types for peanut and soybean crops. They evaluated this approach using a dataset to simulate the impact of velvetbean caterpillar on soybean.

Using the same approach, the purpose of this work was to: (i) develop a disease model extension for the simulation of STB in wheat, to (ii) evaluate the model performance using a dataset from Argentina; and (iii) to conduct a sensitivity analysis for the impact of different disease progress curves on leaf area index and yield using a dataset from Germany.

2. Materials and Methods

2.1. Model Development

Currently the CCW model does not account for competition with weeds, pests or diseases. To solve this problem, modifications of the current CCW version are necessary to include the impact of leaf diseases on final crop yield.

Plant dry matter accumulation and yield can be expressed as a function of leaf area index (LAI), radiation use efficiency and the loss of assimilates due to respiration. Pathogens can modify both leaf area index and daily photosynthesis [35].

The primary damage resulting from STB is defoliation, which reduces both leaf area and leaf photosynthetic rate [36,37].

To apply the damage theory, it was necessary to integrate the pest damage module [32] structure into the current CCW wheat model (Figure 1). These changes included the adding and linkage of the following subroutines to the original version: PEST.for, LINDM.for, PESTCP.for, VEGDM.for and OPPEST.for. A pest damage definition file was created to define the coupling point "leaf area" for the leaf disease STB (Figure 1), where daily damage could be applied to state and rate variables in the model. Percent cumulative leaf area destroyed (PCLA) was chosen as major coupling point in the model.
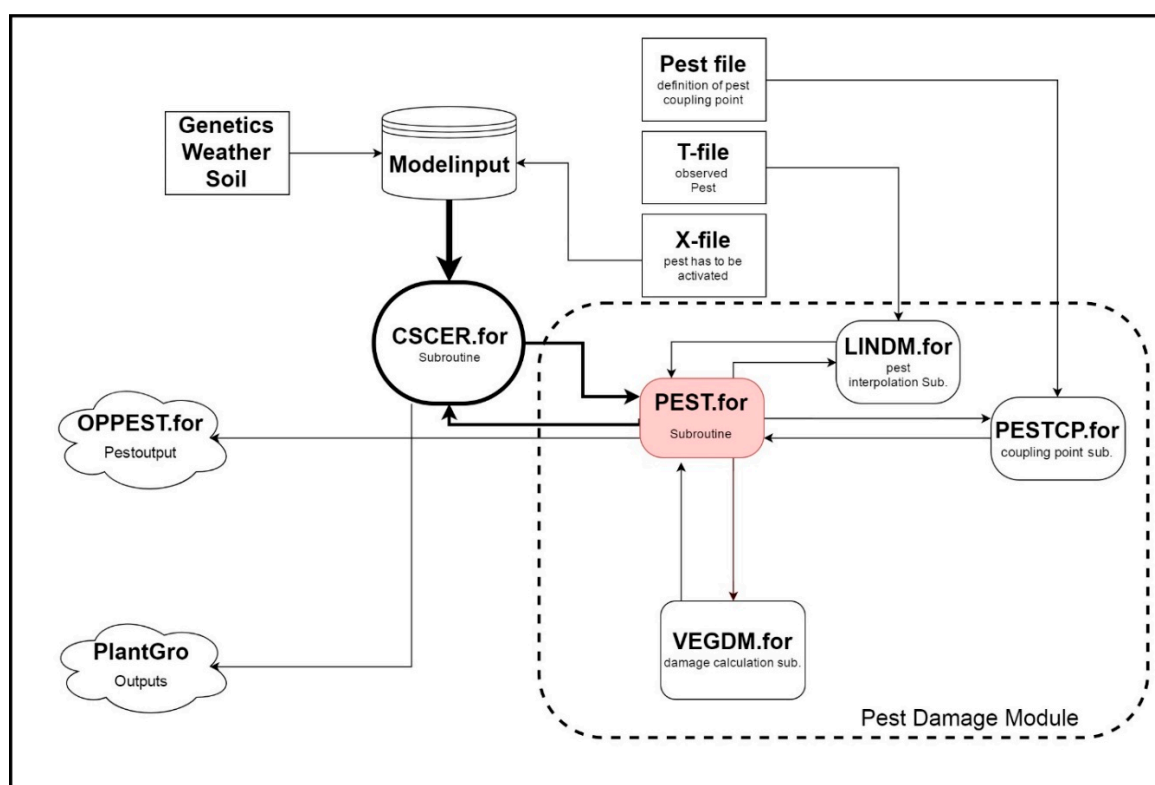
Figure 1. A simplified diagram of the Cropsim-CERES-Wheat (CCW) model with the pest damage module incorporated.

Field observed damage levels were entered in the time series file, referred to as File T in the DSSAT family of models. In this file, the year and day of year (DOY) are entered, along with STB infection in percent. Observed disease infection was linked to the percent cumulative leaf area destroyed (PCLA) coupling point. This damage type (i.e., PCLA) is defined in the pest damage definition model input file, which links field observed damage type and levels to the internal model pest damage coupling point. The model uses a linear interpolation to compute daily damage from periodic field observations. In this work, it was assumed that STB infection began ten days before the first infection symptoms were

observed in the field. This assumption was made, based on Sánchez-Vallet et al. [38] who reported a latent period for STB between day 8 and 14 after infection depending on the environmental conditions. The daily percentage of damage (N_{pt}) was calculated between field observations using

$$N_{pt} = P_{rt*} + \frac{(P_{rt} - P_{rt*})}{(D_{pt} - D_{pt*})} \times (D_s - D_{pt*}) \tag{1}$$

N_{pt} = daily reported damage for damage type p at time t; D_{pt} = DOY of next field observation of damage (P_{rt}); D_{pt*} = DOY of previous field observation of damage (P_{rt*}); D_s = day of current simulation; P_{rt} = damage level reported in the next field observation; P_{rt*} = damage level reported in the previous field observation.

The daily damage calculation, which was applied to the leaf area coupling point (P_{it}) is calculated in the PESTCP. for subroutine (Figure 1) by Equation (2):

$$P_{it} = (N_{pt})(C_{ip}) \tag{2}$$

The pest coefficient (C_{ip}) allows the model to convert units of damage into units used for the model state or rate variable that is being damaged.

After calculating the daily damage to be applied to the diseased leaf area based on interpolations from field observations, the daily damage (D_{ipt}) to be applied to the leaf area state variable (defoliated leaf area) is calculated by the following equation:

$$D_{ipt} = X_{it}{}^* - (Xt_{it} - Xs_{it}) \times \left(1 - \frac{P_{it}}{100}\right) \tag{3}$$

$X_{it}{}^*$ = state or model variable i on day t, before application of damage; X_{it} = state or model variable i on day t, after application of damage; Xt_{it} = cumulative amount of coupling point I; Xs_{it} = cumulative senescence of coupling point I; D_{ipt} = amount of damage applied on state or model variable i on day t; P_{it} = coupling point leaf area.

Finally, the model state or rate variable is adjusted by subtracting the computed defoliation from the leaf area state variable by Equation (4):

$$X_{it} = X_{it}{}^* - D_{ipt} \tag{4}$$

X_{it} = state or model variable i on day t, after application of damage; $X_{it}{}^*$ = state or model variable i on day t, before application of damage; D_{ipt} = amount of damage applied on state or model variable i on day t.

2.2. Field Trials

In this study, datasets from two different locations were used for model development. The first dataset was recorded on the Experimental Station Julio Hirschhorn in La Plata (34°56′ S, 57°57′ W, 15 m above sea level, 16.3 °C average temperature; 946 mm mean annual precipitation) National University of La Plata in Argentina. The second experiment was carried out at the Experimental Station Ihinger Hof (48°44′ N, 8°55′ E; 480 m above sea level, mean annual temperature 9.1 °C and 714 mm mean annual precipitation) University of Hohenheim in Germany.

The trial in Argentina was conducted in two consecutive years (2010 and 2011) and published by Castro and Simón [39]. The objective of this trial was to test the tolerance of ten different Argentinean wheat cultivars (*Triticum aestivum* L.) for STB and to evaluate the disease impact on grain yield and grain quality. The sowing dates were on 15th of July in 2010 and 16th of June in 2011. The soil type was a silty loam. Nitrogen was applied as urea at 100 kg N ha^{-1} at sowing and 80 kg N ha^{-1} at the end of tillering. Three different inoculation levels with *Zymoseptoria tritici* D. were performed. The first level was the control treatment, the second was considered to be a low inoculation level (with 5×10^5

spores mL^{-1} suspension), while the third treatment was considered as high inoculation treatment (5×10^6 spores ml^{-1} suspension). All inoculations were performed at growth stage 22 (beginning of tillering) [40] and at growth stage 39 (flag leaf emergence). For model development weather data (daily temperature, rainfall, solar radiation) from the weather station La Plata ($34°56'$ S, $57°57'$ W), disease severity ratings (%) from three growth stages (GS 39, 60, 82), leaf area index (LAI) which was calculated from the green leaf area (GLAI) plus non-green leaf area (NGLAI), yield, soil properties and management information were collected.

The second trial in Germany was conducted in 2006 using the cultivar Monopol with three inoculation levels (control treatment; low inoculation 50%; high inoculation 100%) of *Zymoseptoria tritici*. Inoculation was imposed by spraying 50% or 100% of a spore suspension (1×10^6 spores per mL, strain CBS 292.69) onto the plots at growth stage 32 [41]. The sowing date was 22nd of October 2005 on a silty clay soil. Nitrogen in form of ammonium nitrate was applied at three growth stages: 100 kg N ha^{-1} at GS 30, 80 kg N ha^{-1} at GS 32 and 40 kg N ha^{-1} at GS 49. The objective of this field trial was to use different vegetation indices to determine the occurrence of plant diseases in winter wheat (*Triticum aestivum* L.). For model sensitivity analysis, data including temperature, rainfall and solar radiation from the weather station Ihinger Hof, as well as growth stages, yield monitoring data, disease severity ratings and the LAI at growth stages GS 31, 34 and 49 were collected. Further information on the trial layout can be found in Gröll [41].

2.3. Model Calibration and Evaluation

The modified CCW model extension was incorporated into the DSSAT 4.6 software. Model inputs were created for both datasets from Argentina and Germany. The dataset from La Plata of 2010, which included phenological, yield, soil data (Table 1) and weather data, was used for calibration to test the ability of the model to simulate the impact of STB on wheat growth and yield.

Table 1. Soil properties for experiments in La Plata and Ihinger Hof used in the simulation.

Location La Plata	Clay Content %	Sand Content %	Silt Content %	LLL *	DUL **	SAT ***
0–30 cm	20.7	28.9	50.4	0.226	0.457	0.561
30–60 cm	20.7	28.9	50.4	0.226	0.457	0.561
60–90 cm	20.7	28.9	50.4	0.226	0.457	0.561
Location Ihinger Hof						
0–30 cm	43.3	9.9	46.8	0.247	0.412	0.467
30–60 cm	43.3	9.9	46.8	0.247	0.412	0.467
60–90 cm	25.0	18.8	56.2	0.142	0.313	0.503

* Lower limit $\hat{=}$ permanent wilting point (pF 4.2). ** Drained upper limit $\hat{=}$ field capacity (pF 1.8). *** Saturated $\hat{=}$ saturated water content (pF 0).

Genetic coefficients for growth and development were calibrated using the 2010 dataset and the control treatment for each cultivar. Calibration was performed by sequentially adjusting the genetic coefficients (Table 2) to minimize the error between measured and simulated values [19]. The existing species file was set as default and the existing ecotype UKWH01 as well as the cultivar file were modified. Coefficients for phenological development (P1V, P1D, P1–P5 and PHINT) were calibrated in the first step, followed by crop growth coefficients (G1, G2 and G3). The RMSE, index of agreement (d-Index) and modelling efficiency (EF) statistics were used to assess the quality of the calibration (see section statistical evaluation). After calibration of individual cultivars, the percentage infection with STB of the low and high inoculation was applied to test the model response. The dataset from La Plata of 2011 was used for model validation.

Table 2. Cultivar coefficients in Cropsim-CERES-Wheat (CCW) model used to simulate crop development, crop growth and crop yield for different cultivars.

Parameter	Definition	Ihinger Hof			La Plata				
		Monopol	ACA801	B75 Aniversario	Buck Brasil	Buck Guapo * Baguette 10 * Klein Zorro * Relmó Centinela *	Klein Escorpion	Klein Flecha	Klein Chaja
		Cultivar file							
P1D	Percentage reduction in development rate in a photoperiod 10 h shorter than the threshold relative to that at the threshold	110	100	100	100	100	100	100	100
P1V	Days at optimum vernalizing temperature required to complete vernalisation	90	20	20	20	20	20	20	20
G1	Kernel number per unit canopy weight at anthesis (kernels g^{-1})	15	25	25	20	22	22	22	25
G2	Standard kernel size under optimum conditions (mg)	48	25	30	30	30	35	30	39
G3	Standard, non-stressed dry weight of a single tiller at maturity (g)	2.0	4.0	4.0	4.0	4.0	4.0	4.0	4.0
P5	Duration of the grain filling phase (°C d)	600	420	430	420	420	420	420	420
PHINT	Interval between successive leaf tip appearances (°C d)	90	92	92	92	92	80	93	92
		Ecotype file							
P1	Duration of phase end juvenile to terminal spikelet	350	350	350	350	350	350	350	350
P2	Duration of phase from double ridges to the end of leaf growth (°C d)	200	250	250	250	250	250	250	250
P3	Duration of phase from the end of leaf growth to the end of spike growth (°C d)	300	220	220	220	220	220	220	220
P4	Duration of phase from the end of spike growth to the end of the grain fill lag (°C d)	380	300	300	300	300	300	300	300
PARUE	Conversion rate from photosynthetically active radiation to dry matter before the last leaf stage (g MJ^{-1})	2.3	2.7	2.7	2.7	2.7	2.7	2.7	2.7
SLAS	Specific leaf area, standard first leaf (cm^2/g)	400	450	450	450	450	450	450	450

* various wheat cultivars with the same cultivar coefficients.

The second dataset from Ihinger Hof was used for sensitivity analysis to test the model on a different location to proof the concept and to test the responsiveness of the model of different STB infection levels. The calibration was performed in the same way as in La Plata with the control treatment by modifying the necessary cultivar coefficients (Table 2). We applied 0%, 10%, 20%, 30%, 50% and 70% damage rates at maximum LAI (GS 39) and started the damage application at growth stage GS 31 to estimate the corresponding yield loss. The different damage rates were used to test the model responsiveness on a broad disease range, which typically starts to impact yield after growth stage 31 [42].

Statistical Evaluation

The statistical model evaluation was conducted by comparing the simulated and observed LAI and yield of the different inoculation treatments (dataset from La Plata).

For statistical analysis, the root mean squared error (RMSE. Equation (5)), the index of agreement (d-Index, Equation (6)) [43] and the modelling efficiency (EF, Equation (7)) were used. The RMSE was used to quantify the amount of variation between simulated and measured values on a metric scale. The d-Index shows if the model is under -or over-estimating the measurements. The EF parameter compares simulated values with the average of the measurements. For a perfect fit between simulated and observed data, the RMSE should be at 0 and the d-Index and EF parameter should have a value of 1.0.

The statistical evaluation was done for simulation runs of the original CCW version and the modified CCW for LAI and yield from both years (2010; 2011) on the location La Plata over all cultivars and inoculation treatments.

Root mean square error (RMSE):

$$RMSE = \left[\frac{1}{n} \sum_{i=1}^{n} (S_i - O_i)^2 \right]^{0.5} \tag{5}$$

Index of agreement (d):

$$d = 1 - \left[\frac{\sum_{i=1}^{n} (S_i - O_i)^2}{\sum_{i=1}^{n} \left(|S_i - \overline{O}| + |O_i - \overline{O}| \right)^2} \right] \tag{6}$$

Modelling efficiency (EF):

$$EF = 1 - \left[\frac{\sum_{i=1}^{n} (S_i - O_i)^2}{\sum_{i=1}^{n} (O_i - \overline{O})^2} \right] \tag{7}$$

where: O_i = observed values; S_i = simulated values; n = numbers of samples; $\overline{O}$ = mean of observed data

3. Results and Discussion

3.1. Model Calibration for La Plata
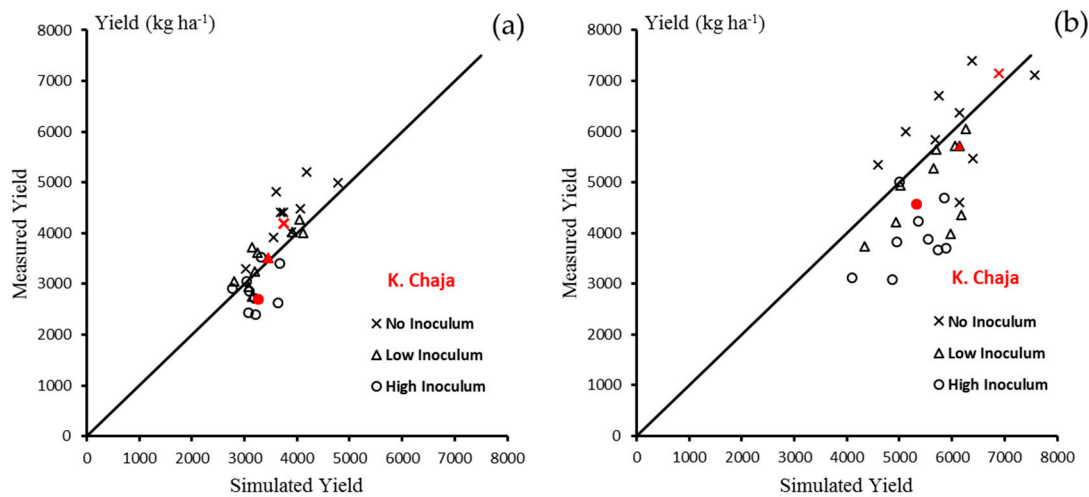
3.1.1. Leaf Area Index

The calibration was performed on the 2010 dataset by fitting the relevant genetic coefficients (Table 2) for phenology and growth. One essential prerequisite for model development is an accurate simulation of growth stages. In this study, growth stages (GS 39; GS 60; GS 82) were predicted by the model conclusively: For all ten cultivars the flowering date (GS 65) was documented approximately 110 days after sowing (DAS), the model simulated this growth stage 115 DAS. A similar result was obtained by comparing observed and simulated DAS of the early dough stage (GS 82) (observed approximately at 131 DAS, simulated 132 DAS).

The main focus of this model calibration was on the adjustment of leaf area as a major coupling point for disease damage. Figures 2 and 3 illustrate the simulated and the observed values for leaf area index and grain yield across different inoculation treatments along with the statistics (Table 3).
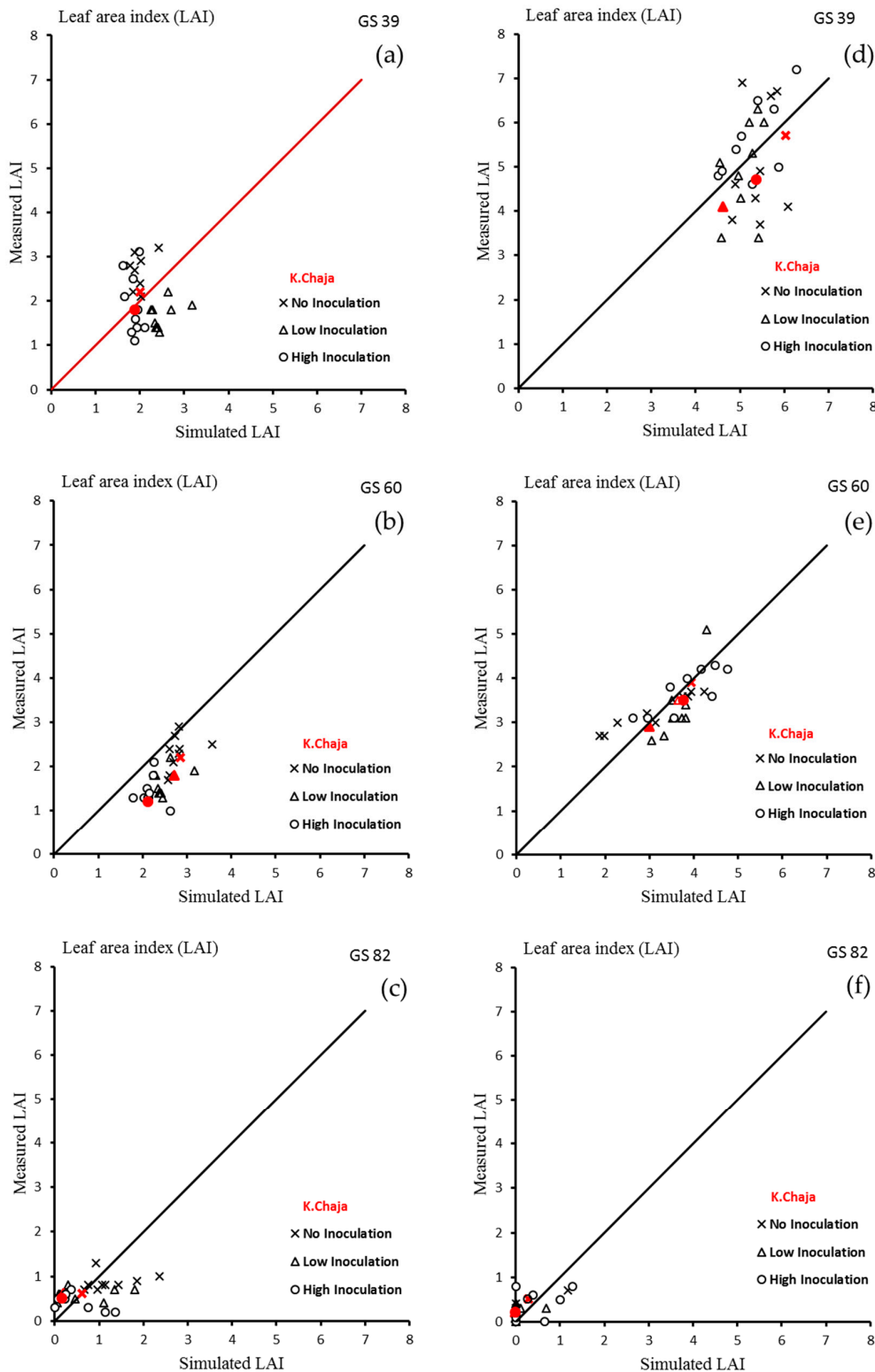
Figure 2. Simulated vs. measured leaf area index (LAI) for calibration (year 2010 **a–c**) and validation (year 2011 **d–f**) for all ten cultivars on the location La Plata. Different symbols represent the different inoculation treatments where × = No Inoculation; Δ = Low Inoculation and O = High Inoculation.

Figure 3. Simulated vs. measured yield (kg DM ha^{-1}) for calibration and validation for all ten cultivars on the location La Plata 2010 (**a**) and La Plata 2011 (**b**).

Table 3. Statistical evaluation of the simulation of leaf area index and grain yield of the original CCW model and the developed CCW model extension for diseases using root mean square error (RMSE), Willmott's d statistic (d-Index) and modelling efficiency (EF).

Variable	Experiment	Original CCW			Modified CCW		
		RMSE	d-Index	EF	RMSE	d-Index	EF
Leaf area index	La Plata 2010	1.19	0.33	−2.69	0.69	0.51	−1.07
	La Plata 2011	2.88	0.24	−0.98	1.11	0.70	0.68
Yield	La Plata 2010	1144	0.47	−1.19	499	0.81	0.58
	La Plata 2011	1755	0.50	−1.19	1285	0.66	−0.18

For demonstration of the overall model behaviour in regard to LAI changes induced by three different STB inoculation treatments over time, the wheat cultivar K. Chaja was selected. This cultivar was considered to be highly susceptible to STB infection [39]. Figure 4a shows the impact of disease infestation on LAI according to different inoculation treatments 90 days after sowing. All three simulation runs reached the maximum LAI at day 100. For the control treatment a maximum LAI of 3.5 was simulated. A difference of 0.5 LAI was found between the control and the high-inoculation treatment. Comparing simulated and observed LAI values, the model predicted the LAI over the vegetation period in an accurate manner (RMSE 0.47, d-Index 0.9).

Similar results are displayed in Figure 2a–c, which illustrates the simulated versus observed LAI across three different inoculation treatments for different cultivars. Regardless of susceptibility, in GS 39 all ten cultivars showed a homogenous distribution of all data points around the 1:1 line with no strong outliers. A slight tendency for an overestimation of LAI was given at GS 39 in the low and high inoculation treatments, whereas for the control treatment a slight underestimation was shown over all cultivars. In GS 60 and GS 82, a slight overestimation of LAI was found for all inoculation treatments.
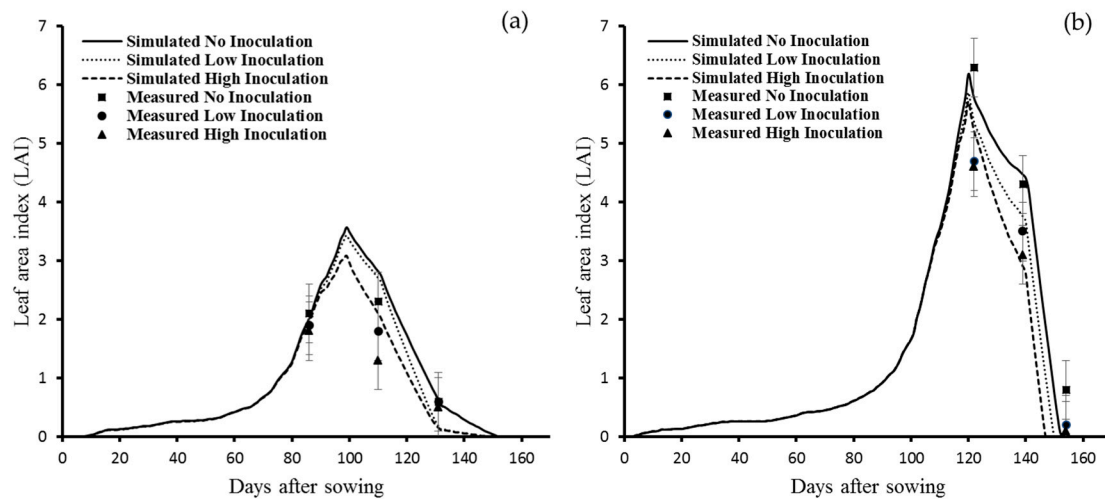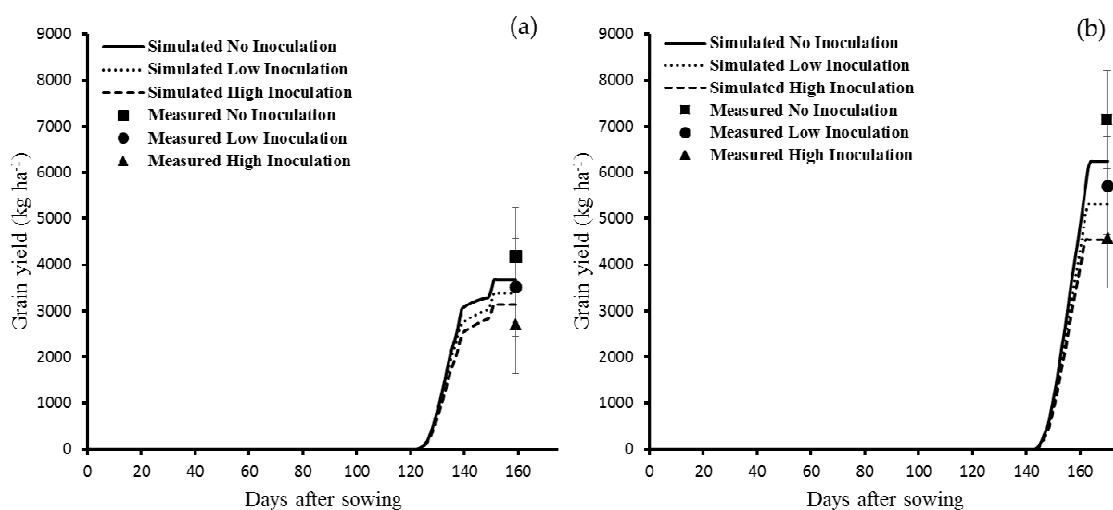
Figure 4. Simulated and measured leaf area index values for cultivar K. Chaja, year 2010 (**a**) and 2011 (**b**) including different inoculation treatments with septoria tritici blotch (STB). The error bars demonstrate the LSD of the leaf area index.

Finally, the modified CCW model (RSME 0.69; d-Index 0.51) performed better compared to the original CCW model (RSME 1.19; d-Index 0.33), as indicated by the corresponding statistics. Outliers in Figure 2a–c can be explained by the LSD ranging from 0.4 to 1.0 depending on the sampling date, reported from Castro and Simón [39].

Nevertheless, the model was able to account for all ten cultivars representing different tolerance levels to STB at different growth stages and disease severities accurately.

3.1.2. Yield

A reduction in LAI after infection with STB also leads to a reduction in yield (Figure 5a). Yield formation started for the cultivar K. Chaja (Figure 5a) on day 122 and was negatively correlated with the inoculation treatment. Yield of the control treatment (3800 kg ha^{-1}) was slightly underestimated and the high inoculation treatment (3400 kg ha^{-1}) showed a slight overestimation.

Figure 5. Simulated and measured grain yield values for cultivar K. Chaja year 2010 (**a**) and 2011 (**b**) including different inoculation treatments with STB. The error bars demonstrate the LSD of the yield.

Figure 3a represents the observed versus the simulated yield for all ten cultivars and showed a dense clustering of the different inoculation treatments around the 1:1 line. Overall, it indicated

the highest simulated yield for the control and the lowest yield for the high inoculation treatment. The results illustrated the capability of the modified CCW model to account for disease damage. This is expressed in the statistical evaluation (Table 3), where a reduction of the RMSE from 1144 (original version) to 499 (modified version) was observed. The d-Index also underlined these findings, which increased from 0.47 (original version) to 0.81 (modified version).

The modification of the existing CCW showed very good results in LAI and yield simulation (Table 3). It indicated a clear improvement for all statistical parameters compared with the existing CCW included in the current DSSAT version. The calibration successfully minimized the error between measured and simulated data for both, LAI and yield.

3.2. Model Validation for La Plata

3.2.1. LAI

Illustrating LAI (Figure 2d–f) and yield (Figure 3b) for the cultivar K. Chaja and all cultivars in the validation year 2011.

In 2011, a maximum LAI of 6.3 was observed in the control treatment for K. Chaja (Figure 4b) at day 120. The model simulated a maximum LAI of 6.2 for the control treatment on the same day. For the low-inoculation treatment, a maximum LAI of 4.7 was observed, whereas the model simulated a maximum LAI of 5.8. Regarding the highest inoculation treatment, a LAI of 4.6 was observed in the field experiment. The model simulated for the same treatment a maximum LAI of 5.7. The model was capable to simulate the maximum LAI for the control treatment exactly but it slightly overestimated the maximum LAI both for the lowest and highest inoculation treatment.

In general LAI was higher in 2011 than in 2010 independent of cultivars, growth stages and inoculation treatments (Figure 2). For 2011 and GS 39, the 1:1 plot showed no strong outliers and a slight overestimation for the control treatment and a slight underestimation for the highest inoculation treatment. This can be caused by an earlier onset of disease in the inoculated treatments which was not reported and cause a slightly underestimation in the model. For GS 60 and GS 82 the model predicted the observed LAI values accurately.

3.2.2. Yield

Yield formation started 140 days after sowing for K. Chaja (Figure 5b), while full maturity was reached on day 165. A maximum yield of 6000 kg ha^{-1} was reached in the control treatment compared with the lowest yield of 5400 kg ha^{-1} in the high inoculation treatment. The corresponding error bars of the measured values were met by the simulated curves, which indicated a high accuracy of the simulation. Under consideration of all cultivars and inoculation treatments (Figure 3b) data points scattered around the 1:1 line on a broader range compared to the calibration (Figure 3a). An inverse relationship between inoculation level and yield was shown (Figure 5).

Overall, the developed model extension was able to account for STB disease damage. This is also shown by the statistics (Table 3), where a 30% improvement of the RMSE in the modified CCW version was achieved compared with the original model. This improvement was also shown by the d-Index and EF values. Further, the calibration showed a higher model accuracy when compared with the validation. Jing et al. [44] and Attia et al. [45] also reported a slightly weaker simulation accuracy regarding the validation dataset.

For 2010, a 20 days shorter growing period due to a 30 days later sowing date and a 130 mm lower precipitation compared to 2011 [39] was reported. Both factors resulted in a reduction of LAI and yield in 2010. Despite these differences the model performed very well for each inoculation treatment and showed its robustness when growing conditions differ between years. Measured yields in the inoculation treatments were simulated quite accurately, while the measured mean value of the control showed a 5% off-set. An explanation for this offset might be given in the way the disease ratings were performed and represented in the model. The model used the mean values from the disease

ratings of all repetitions and did not represent each individual plot. It is also possible that the trials had a slight infection of other diseases, which were not measured and caused a slight model offset. Another conceivable reason is the defined onset of disease ten days before disease rating was reported. This assumption was made because of the reported latent period for STB between day 8 and 14 after infection from Sánchez-Vallet et al. [38].

For 2010 and 2011, the d-Index values of the original CCW version are in a similar range for both LAI and yield. In the developed model extension, the d-Index, which represents the model accuracy, increased strongly even though in different intensities for each year. This may point to one possible shortcoming of the current model extension, as it does not account for spore disposal [46]. Spore disposal model use different leaf layers, rain intensity thresholds, droplets, sporulation and concentrations of starting spore pools and can therefore extend the simulation accuracy further.

Nevertheless, other STB models show a strong performance, if a minimum dataset is provided, in which more inputs like leaf wetness are included [47] or in which the initial state of infection of the first leaves is known [46]. Magarey et al. [47] also reported the necessity of hourly weather data for many disease models. In previous datasets this information is not given [48] and they cannot be used for disease modelling, which is literally a loss of information for agricultural decision making. This clearly shows the advantage of the developed CCW extension, in which only the percentage of disease rating, weather- and soil data is needed as a minimum dataset. This leads to a more accurate simulation as shown in Table 3 and makes the CCW applicable for a broader use.

3.3. Sensitivity Analysis

In order to test the general responsiveness of the developed model extension, a sensitivity analysis was carried out by comparing different inoculation treatments with the corresponding disease infections [41]. The model was calibrated by using an independent dataset with disease infections from Germany [41]. The disease infections varied between 4%, 13% and 15%. Disease infection started in GS 31 (DAS 200). Figure 6a depicts the simulated curves for the three different inoculation treatments. A maximum LAI of 7.3 was reached 40 days after GS 31. Simulated curves illustrate a clear separation between the 4%, 13% and the 15% disease infection. A maximum LAI of 7.2, 6.3, 6.1 was reached at day 240 at 4%, 13% and the 15% disease infection rating. Comparing simulated infection scenarios with measured values, the model simulated the LAIs of the three different disease infection levels accurately.
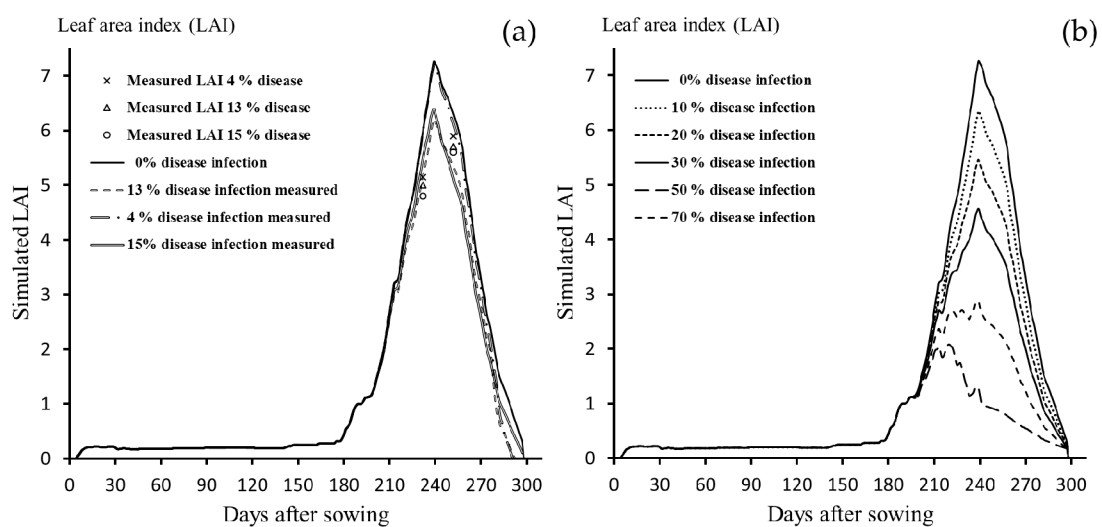
Figure 6. Sensitivity analysis of the CCW disease extension for measured disease infections (4%; 13%; 15%) (**a**) and for five infection scenarios (0%; 10%; 20%; 30%; 50%; 70% disease infection) (**b**) with STB at the location Ihinger Hof.

In the next step an artificial disease infection level of up to 70% was applied (Figure 6b) to test the general responsiveness and the boundaries of the developed model and to test the leaf damage theory on the leaf area coupling point (PCLA).

In Figure 6a a maximum LAI of 7.3 was reached 40 days after GS 31 in the control treatment. LAI increased almost linearly from day 200 to day 240 before the onset of senescence led to a constant decrease in LAI up to final harvest date. For the depicted disease infection scenarios of 10%, 20%, 30% and 50 % a maximum LAI of 7.3, 6.2, 5.4, 4.6, 2.9 and 1.3 was reached at day 240 (Figure 6b). The 70% disease infection scenario showed that a maximum LAI of 2.0 was reached earlier at 220 DAS (Figure 6b). Due to the massive destruction of leaf area, a shortage of assimilate production occurred, which affected in a next step the growth of new leaves. Simulated LAI reduction for maximum LAI in the different disease levels followed the magnitude of 12.5 % (10% diseased LAI), 24.8% (20% diseased LAI), 37.1% (30% diseased LAI), 60.3% (50% diseased LAI) and 82.4% (70% diseased LAI) (Table 4).

Table 4. Yield evaluation of the sensitivity analysis from the Ihinger Hof dataset, by comparing the percentage disease infection with STB and the corresponding simulated percentage yield reduction in kg DM ha^{-1} for the cultivar Monopol.

% Disease Infection	Simulated Yield kg ha^{-1}	Measured Yield kg ha^{-1}	% Yield Reduction	% LAI Reduction at Maximum LAI
0	4384		0	0
4 *	4332	4409	1.2	0.8
10	4190		4.4	12.5
13 *	4159	3934	5.1	14.5
15 *	4124	3965	5.9	12.0
20	3990		9.0	24.8
30	3737		14.8	37.1
50	3242		26.0	60.3
70	2380		45.7	82.4

* measured disease infection.

Table 4 shows the corresponding yields of the applied and measured disease infection levels. The maximum observed yield obtained with the disease infection level of 4% was 4409 kg ha^{-1}. Higher disease infection levels (13%; 15%) resulted in lower yield (3934 kg ha^{-1}; 3965 kg ha^{-1}). Simulated yield decreased gradually with higher infection levels. The control treatment resulted in a maximum yield of 4384 kg ha^{-1}, while the 70% disease infection level resulted in a total grain yield of 2380 kg ha^{-1} which corresponded to a 45.7% yield reduction. Over all tested disease infection levels, the simulated yield reduction followed an exponential shape, indicating that yield reductions became more severe and are more than doubled at higher disease infection levels. An exponential relationship between yield loss and disease infection was also shown by King et al. [49].

Comparing simulated and measured yield, the model showed a slightly underestimation for the 4% level and a slight overestimation for the 13% and 15% disease infection level. These variations are in an acceptable range.

Regarding the accuracy of the current simulation, similar results for yield reduction based on the occurrence of leaf diseases are reported by Ziv and Eyal [50]. Ziv and Eyal [50] tested different inoculation treatments in different spring wheat cultivars and reported yield losses of up to 53% at a disease infection of 73%. The developed CCW model extension gave comparable results to a previous study of Bhathal et al. [51] also at lower infection level scenarios. Bhathal et al. [51] tested different inoculation treatments in wheat to evaluate the relationship between disease infection and yield. Notably, they showed an onset of the disease as it was used in the sensitivity analysis of this study, at GS 31 and demonstrated a 10% yield loss due to a natural disease infection of 26%. King et al. [49], also confirmed this model theory on an independent dataset from the United Kingdom carried out at four different locations. Similar observations and an exponential yield loss curve due to STB disease were obtained. In addition, a yield loss of 30% by a disease infection of 55.1% as well as a yield

reduction of 8% by a disease infection of 14.5% occurred. This confirmed the model theory and clearly showed the capability to simulate leaf disease infection with STB by using the coupling point leaf area (PCLA).

3.4. Future Model Applications

Despite the good simulation results, the developed model concept can currently only be used for STB. The concept was not tested on other wheat diseases like stripe rust caused by "*Puccinia striiformis* W.," stem or black rust caused by "*Puccinia graminis* E." or powdery mildew caused by "*Blumeria graminis* P." It can be assumed that this concept will also work for other diseases, by changing the pest coefficient in the pest file to account for different damage types. Bastiaans [52] showed a ß–value for STB, which represents the correlation between visible affected leaf area and the affected photosynthetic rate. A ß–value > 1 indicates a stronger effect on photosynthetic rate as it visually appears. For STB this value is close to 1 wherefore the pest coefficient in the CCW model extension was set to 1. Bastiaans [52] reported a ß–value of 8.7 for "*Erisyhe graminis*" or 1.3 for "*Puccinia recondita*" in winter wheat. It is assumed, that the pest coefficient has to be increased in a similar manner but it has to be proven by real data. However, the structure of the model extension is set up in a flexible way and has the possibility to be transferred to other leaf diseases.

Further, the disease extension routine can suite as a gateway between crop models and remote sensing data, like it was published by Thorp et al. [53]. Thorp et al. [53] showed an improvement of simulation results by updating the plant leaf area state variable with green LAI generated by remote sensing. This offers the opportunity to simulate a given field on a site-specific scale, which means the CCW model extension can be updated by the percentage diseased leaf area detected by for example, remote sensing. In this way, the model could serve as decision support tool to give farmers an economic advise on a field level as Ficke et al. [54] proposed.

4. Conclusions

In this study a disease extension for the CCW model was developed to simulate the damage effect of STB disease on LAI and yield in wheat. The model was tested successfully in a sensitivity analysis on a German dataset and on a dataset obtained from La Plata, Argentina. Results of the study clearly showed the effect of the implementation of the coupling point "PCLA" and on the corresponding LAI and yield for different locations. For the location La Plata, the obtained simulation results of the modified CCW model indicated a higher model accuracy which almost doubled and clearly showed an improved model behaviour. Especially for the cultivar K. Chaja, the CCW model extension showed a high modelling accuracy. The LAI and yield were simulated very accurate in both years. Furthermore the sensitivity analysis also displayed the flexibility of the CCW model extension to account for disease damage over a broad range between 0 and 70% of STB disease infection.

Nevertheless, further research is needed to test the developed model on other leaf diseases like leaf rust, powdery mildew or stripe rust in wheat. The model extension could be used in future studies as decision support system for example, coupled with remote sensing technologies to obtain the necessary disease ratings for the model input files.

Conflicts of Interest: The authors declare no conflict of interest. The funders had no role in the design of the study; in the collection, analyses or interpretation of data; in the writing of the manuscript or in the decision to publish the results.

References

1. Singh, R.P.; Singh, P.K.; Rutkoski, J.; Hodson, D.P.; He, X.; Jørgensen, L.N.; Hovmøller, M.S.; Huerta-Espino, J. Disease Impact on Wheat Yield Potential and Prospects of Genetic Control. *Annu. Rev. Phytopathol.* **2016**, *54*, 303–322. [CrossRef] [PubMed]
2. Olesen, J.E.; Trnka, M.; Kersebaum, K.C.; Skjelvåg, A.O.; Seguin, B.; Peltonen-Sainio, P.; Rossi, F.; Kozyra, J.; Micale, F. Impacts and adaptation of European crop production systems to climate change. *Eur. J. Agron.* **2011**, *34*, 96–112. [CrossRef]
3. Eigenbrode, S.D.; Binns, W.P.; Huggins, D.R. Confronting Climate Change Challenges to Dryland Cereal Production: A Call for Collaborative. *Prod. Engagem.* **2018**, *5*. [CrossRef]
4. Ahanger, R.A.; Bhat, H.A.; Bhat, T.A.; Ganie, S.A.; Lone, A.A.; Wani, I.A.; Ganai, S.A.; Haq, S.; Khan, O.A.; Junaid, M.J.; Bhat, T.A. Impact of Climate Change on Plant Diseases. *Int. J. Modern Plant & Anim. Sci. USA* **2013**, *3*, 105–115.
5. Weiss, M.V. *Compendium of Wheat Diseases*, 2nd ed.; APS Press: St. Paul, MN, USA, 1987.
6. Forrer, H.R.; Zadoks, J.C. Yield reduction in wheat in relation to leaf necrosis caused by Septoria tritici. *Neth. J. Plant Pathol.* **1983**, *89*, 87–98. [CrossRef]
7. Eyal, Z. The septoria tritici and stagonospora nodorum blotch diseases of wheat. *Eur. J. Plant Pathol.* **1999**, *105*, 629–641. [CrossRef]
8. Bearchell, S.J.; Fraaije, B.A.; Shaw, M.W.; Fitt, B.D.L.; Cowling, E.B. Wheat Archive Links Long-Term Fungal Pathogen Population Dynamics to Air Pollution. *Proc. Natl. Acad. Sci. USA* **2005**, *102*, 5438–5442. [CrossRef] [PubMed]
9. Eyal, Z.; Amiri, Z.; Wahl, I. Physiological Specialization of Septoria tritici. *Phytopathology* **1973**, *63*, 1087–1091. [CrossRef]
10. Fones, H.; Gurr, S. The impact of Septoria tritici Blotch disease on wheat: An EU perspective. *Fungal Genet. Biol.* **2015**, *79*, 3–7. [CrossRef] [PubMed]
11. Fraaije, B.; Cools, H.J.; Fountaine, J.; Lovell, D.J.; Motteram, J.; West, J.S.; Lucas, J. A Role of Ascospores in Further Spread of QoI-Resistant Cytochrome b Alleles (G143A) in Field Populations of Mycosphaerella graminicola. *Phytopathology* **2005**, *95*, 933–941. [CrossRef] [PubMed]
12. Estep, L.K.; Torriani, S.F.F.; Zala, M.; Anderson, N.P.; Flowers, M.D.; Mcdonald, B.A.; Mundt, C.C.; Brunner, P.C. Emergence and early evolution of fungicide resistance in North American populations of Zymoseptoria tritici. *Plant Pathol.* **2015**, *64*, 961–971. [CrossRef]
13. Simón, M.R.; Cordo, C.A.; Castillo, N.S.; Struik, P.C.; Börner, A. Population Structure of Mycosphaerella graminicola and Location of Genes for Resistance to the Pathogen: Recent Advances in Argentina. *Int. J. Agron.* **2012**, *2012*, 680275. [CrossRef]
14. Rodrigo, S.; Cuello-Hormigo, B.; Gomes, C.; Santamaria, O.; Costa, R.; Poblaciones, M.J. Influence of fungicide treatments on disease severity caused by Zymoseptoria tritici, and on grain yield and quality parameters of bread-making wheat under Mediterranean conditions. *Eur. J. Plant Pathol.* **2014**, *141*, 99–109. [CrossRef]
15. Keating, B.A.; Carberry, P.S.; Hammerb, G.L.; Probert, M.E.; Robertson, M.J.; Holzworth, D.; Huth, N.I.; Hargreaves, J.N.G.; Meinke, H.; Hochman, Z.; et al. An overview of the crop model APSIM. *Eur. J. Agron.* **2003**, *18*, 267–288. [CrossRef]
16. Lv, Z.; Liu, X.; Cao, W.; Zhu, Y. Agricultural and Forest Meteorology Climate change impacts on regional winter wheat production in main wheat production regions of China. *Agric. For. Meteorol.* **2013**, *171–172*, 234–248. [CrossRef]
17. Brisson, N.; Gary, C.; Justes, E.; Roche, R.; Mary, B.; Ripoche, D.; Zimmer, D.; Sierra, J.; Bertuzzi, P.; Burger, P.; et al. An overview of the crop model Stics. *Eur. J. Agron.* **2003**, *18*, 309–332. [CrossRef]
18. Jamieson, P.D.; Semenov, M.A.; Brooking, I.R.; Francis, G.S. Sirius a mechanistic model of wheat respinse to environmental variation. *Eur. J. Agron.* **1998**, *8*, 161–179. [CrossRef]

19. Jones, J.W.; Hoogenboom, G.; Porter, C.H.; Boote, K.J.; Batchelor, W.D.; Hunt, L.A.; Wilkens, P.W.; Singh, U.; Gijsman, A.J.; Ritchie, J.T. The Dssat Cropping System Model. *Eur. J. Agron.* **2003**, *18*, 235–265. [CrossRef]

20. Hunt, L.A.; Pararajasingham , S. CROPSIM—WHEAT: A model describing the growth and development of wheat. *Can. J. Plant Sci.* **1995**, 619–632.

21. Ritchie, J.T.; Singh, U.; Godwin, D.C.; Bowen, W.T. Cereal growth, development and yield. *Underst. Opt. Agric. Prod.* **1998**, 79–98. [CrossRef]

22. Ritchie, J.T.; Otter, S. Description and performance of CERES-Wheat: A user-orientes wheat yield model. *ARS Wheat Yield Proj.* **1985**, *38*, 159–175.

23. Hoogenboom, G.; Jones, J.W.; Wilkens, P.W.; Porter, C.H.; Boote, K.J.; Hunt, U.S.; Lizaso, J.I.; White, J.W.; Uryasev, O.; Ogoshi, R.; et al. *Decision Support System for Agrotechnology Transfer (DSSAT) [CD-ROM]*; University of Hawaii: Honululu, HI, USA, 2015.

24. Thorp, K.R.; Hunsaker, D.J.; French, A.N.; White, J.W.; Clarke, T.R. Evaluation of the CSM-CROPSIM-CERES-Wheat Model as a Tool for Crop Water Management. *Trans. ASABE* **2010**, *53*, 1–17. [CrossRef]

25. Chipanshi, A.C.; Ripley, E.A.; Lawford, R.G. Large-scale simulation of wheat yields in a semi-arid environment using a crop-growth model. *Agric. Syst.* **1999**, *59*, 57–66. [CrossRef]

26. Savin, R.; Satorre, E.H.; Hall, A.J.; Slafer, G.A. Assessing strategies for wheat cropping in the monsoonal climate of the Pampas using the CERES-Wheat simulation model. *Field Crops Res.* **1995**, *42*, 81–91. [CrossRef]

27. Sardinia, S.; Dettori, M.; Cesaraccio, C.; Motroni, A.; Spano, D.; Duce, P. Field Crops Research Using CERES-Wheat to simulate durum wheat production and phenology. *Field Crops Res.* **2011**, *120*, 179–188. [CrossRef]

28. Bannayan, M.; Crout, N.M.J.; Hoogenboom, G. Application of the CERES-Wheat model for within-season prediction of winter wheat yield in the United Kingdom. *Agron. J.* **2003**, *95*, 114–125. [CrossRef]

29. Gbegbelegbe, S.; Cammarano, D.; Asseng, S.; Robertson, R.; Chung, U.; Adam, M.; Abdalla, O.; Payne, T.; Reynolds, M.; Sonder, K.; et al. Baseline simulation for global wheat production with CIMMYT mega-environment specific cultivars. *Field Crops Res.* **2017**, *202*, 122–135. [CrossRef]

30. Batchelor, W.D.; Jones, J.W.; Boote, K.J.; Porter, C.H. *Pest and Disease Damage Module*; University of Florida: Gainsville, FL, USA, 2004.

31. Boote, K.J.; Bennet, J.M.; Jones, J.W.; Jowers, H.E. On-farming testing of peanut and soybean models in north Florida. *Paper Am. Soc. Agric. Eng. USA* **1989**. Available online: http://agris.fao.org/agris-search/search.do?recordID=US9165910 (accessed on 10 January 2019).

32. Batchelor, W.D.; Jones, J.W.; Boote, K.J.; Pinnschmidt, H.O. Extending the use of crop models to study pest damage. *Trans. Am. Soc. Agric. Eng. Gen. Ed.* **1993**, *36*, 551–558. [CrossRef]

33. Boote, K.J.; Jones, J.W.; Hoogenboom, G.; Pickering, N.B. The CROPGRO model for grain legumes. In *Understanding Options for Agricultural Production*; Tsuji, G.Y., Hoogenboom, G., Thornton, P.K., Eds.; Springer: Dordrecht, The Netherlands, 1998; pp. 99–128. ISBN 978-94-017-3624-4.

34. Andarzian, B.; Hoogenboom, G.; Bannayan, M.; Shirali, M.; Andarzian, B. Determining optimum sowing date of wheat using CSM-CERES-Wheat model. *J. Saudi Soc. Agric. Sci.* **2015**, *14*, 189–199. [CrossRef]

35. Waggoner, P.E.; Berger, R.D. Defoliation, Disease, and Growth. *Phytopathology* **1987**, *77*, 1495–1497.

36. Robert, C. Analysis and modelling of effects of leaf rust and Septoria tritici blotch on wheat growth. *J. Exp. Bot.* **2004**, *55*, 1079–1094. [CrossRef] [PubMed]

37. Robert, C.; Bancal, M.O.; Lannou, C.; Ney, B. Quantification of the effects of Septoria tritici blotch on wheat leaf gas exchange with respect to lesion age, leaf number, and leaf nitrogen status. *J. Exp. Bot.* **2006**, *57*, 225–234. [CrossRef] [PubMed]

38. Sánchez-Vallet, A.; McDonald, M.C.; Solomon, P.S.; McDonald, B.A. Is Zymoseptoria tritici a hemibiotroph? *Fungal Genet. Biol.* **2015**, *79*, 29–32. [CrossRef] [PubMed]

39. Castro, A.C.; Simón, M.R. Effect of tolerance to Septoria tritici blotch on grain yield, yield components and grain quality in Argentinean wheat cultivars. *Crop Prot.* **2016**, *90*, 66–76. [CrossRef]

40. Zadoks, J.C.; Chang, T.T.; Konzak, C.F. A decimal code for the growth stages of cereals. *Weed Res.* **1974**, *14*, 415–421. [CrossRef]

41. Gröll, K. *Use of Sensor Technologies to Estimate and Assess the Effects of Various Plant Diseases on Crop Growth and Development*; Universty of Hohenheim: Stuttgart, Germany, 2008; Available online: http://opus.uni-hohenheim.de/volltexte/2008/296/ (accessed on 10 January 2019).

42. Thomas, M.; Cook, R.; King, J. Factors affecting development of Septoria tritici in winter wheat and its effect on yield. *Plant Pathol.* **1989**, 246–257. [CrossRef]

43. Willmott, C.J. Some Comments on the Evaluation of Model Performance. *J. Appl. Phys.* **1982**, *36*, 1309–1313. [CrossRef]

44. Jing, Q.; Qian, B.; Shang, J.; Huffman, T.; Liu, J.; Pattey, E.; Dong, T.; Tremblay, N.; Drury, C.F.; Ma, B.L.; et al. Assessing the options to improve regional wheat yield in eastern canada using the csm–ceres–wheat model. *Agron. J.* **2017**, *109*, 510–523. [CrossRef]

45. Attia, A.; Rajan, N.; Xue, Q.; Nair, S.; Ibrahim, A.; Hays, D. Application of DSSAT-CERES-Wheat model to simulate winter wheat response to irrigation management in the Texas High Plains. *Agric. Water Manag.* **2016**, *165*, 50–60. [CrossRef]

46. Robert, C.; Fournier, C.; Andrieu, B.; Ney, B. coupling a 3D virtual wheat (Triticum aestivum) plant model with a Septoria tritici epidemic model (Septo3D): A new approach to investigate plant-pathogen interactions linked to caonpy architecture. *Funct. Plant Biol.* **2008**, *35*, 997–1013. [CrossRef]

47. Magarey, R.D.; Sutton, T.B.; Thayer, C.L. A Simple Generic Infection Model for Foliar Fungal Plant Pathogens. *Phytopathology* **2005**, *95*, 92–100. [CrossRef] [PubMed]

48. Donatelli, M.; Magarey, R.D.; Bregaglio, S.; Willocquet, L.; Whish, J.P.M.; Savary, S. Modelling the impacts of pests and diseases on agricultural systems. *Agric. Syst.* **2017**, *155*, 213–224. [CrossRef] [PubMed]

49. King, J.E.; Jenkins, J.E.E.; Morgan, W.A. The estimation of yield losses in wheat from severity of infection by Septoria species. *Plant Pathol.* **1983**, *32*, 239–249. [CrossRef]

50. Ziv, O.; Eyal, Z. Assessment of Yield Component Losses Caused in Plants of Spring Wheat Cultivars by Selected Isolates of Septoria tritici. *Phytopathology* **1977**, *68*, e796. [CrossRef]

51. Bhathal, J.S.; Loughman, R.; Speijers, J. Yield reduction in wheat in relation to leaf disease from yellow (tan) spot and septoria nodorum blotch. *Eur. J. Plant Pathol.* **2003**, *109*, 435–443. [CrossRef]

52. Bastiaans, L. Ecology and Epidemiology Ratio Between Virtual and Visual Lesion Size as a Measure to Describe Reduction in Leaf Photosynthesis of Rice Due to Leaf Blast. *Phytopathology* **1991**, *81*, 611–615. [CrossRef]

53. Thorp, K.R.; Hunsaker, D.J.; French, A.N. Assimilating leaf area index estimates from remote sensing into the simulations of a cropping systems model. *Trans. ASABE* **2010**, *53*, 251–262. [CrossRef]

54. Ficke, A.; Cowger, C.; Bergstrom, G.; Brodal, G. Understanding Yield Loss and Pathogen Biology to Improve Disease Management: Septoria Nodorum Blotch—A Case Study in Wheat. *Plant Dis.* **2018**, *102*, 696–707. [CrossRef] [PubMed]